Proceedings of 2014 IEEE
International Conference on Mechatronics and Automation
August 3 - 6, Tianjin, China

Global Path Planning with Obstacle Avoidance for Omnidirectional Mobile Robot Using Overhead Camera

Zahra Ziaei, Reza Oftadeh, and Jouni Mattila
Department of Intelligent Hydraulics and Automation (IHA)
Tampere University of Technology
Tampere, Finland.
{*zahra.ziaei, reza.oftadeh, jouni.mattila*}*@tut.fi*

***Abstract*—Path planning is one of the indispensable modules of autonomous mobile robots that delineates a collision-free path between two desired positions in an obstacle-cluttered workspace. In this paper, we propose a global path planning method in the image plane using a single overhead camera based on the principle of artificial potential fields. Our algorithm optimally fuses an image-based technique for obstacle avoidance with path planning in the image space and integrates the CAD-based recognition method. The proposed method is suitable for planning the desired path for the omnidirectional mobile robots, and it is used as an input to our previously developed path-following controller. Experiment results show the efficiency of the generated path using an overhead camera for the omnidirectional robot iMoro which is a four-wheeled, independently steered mobile robot.**

***Index Terms*—Path Planning, Obstacle Avoidance, Mobile Robot, Image Space, Overhead Camera.**

I. Introduction

The goal of a navigation system is to direct an autonomous mobile robot from an initial configuration to a final desired pose without getting lost or colliding with other objects in the environment. The basic mobile robot navigation can be divided into three main tasks as follows [1]:

- Generate a model or map of the environment.
- Compute an obstacle-free path from start pose to goal.
- Traverse the generated trajectory in the workspace.

Between these main tasks, the path planning algorithm is one of the most important issues. To this end, the modeling or mapping the static or dynamic environment is another necessary task. There are manifold of path planning algorithms with obstacle avoidance in the literature [2]. Find-path problem in the plane is well known in robotics and plays a vital role in the navigation of autonomous mobile robots. The path planning component is divided into two categories: global path planning and local path planning. Global path planning can plan an initial route from the mobile robot's current position to the target position based on the prior global map. Local path planning is based on sensory information in uncertain environments in which the global positions of the obstacles are unknown [2].

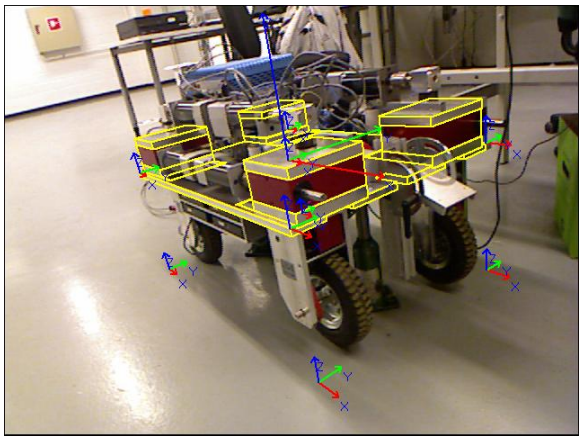

Fig. 1. A view of the mobile robot (iMoro) [8] and its body frame and vertices poses in the image space using the CAD-based method [9].

The Artificial Potential Field (APF) method [3] is one of the most popular approaches used to navigate mobile robots within environments containing obstacles. The APF was originally developed as an on-line collision avoidance for local path planners [3].

The global path planning technique based on the APF was defined in [4] to provide stationary obstacle avoidance and path planning for the mobile robots and revolutes manipulator. The major problem in the real-time path planning using APF method is the local minimum issue, which can make a trap for a robot before reaching its goal location. However, by considering the entire path in the global path planning using APF method, the local minimum problem is greatly reduced, allowing the method to be used for global path planning [4].

A predefined map of the robot workspace is necessary to generate an optimal obstacle-free path in the global path planning method [5]. An overhead camera can be used to map the 3D environments into 2D image model, i.e., for planning a path [6] or modeling the system as a differentially flat system, which relies on waypoints specified in the image space [7]. The image-based path planning for camera-in-hand visual servoing has been introduced in [10]. By integrating the image-based path planning and the CAD-based recognition

978-1-4799-3979-4/14/$31.00 ©2014 IEEE

method, [11] extends this approach for 3D visual servoing manipulation.

In this paper, the said approach is advanced to plan a path for an omnidirectional mobile robot [8] using a fixed overhead camera. To this end, the image-based path planing method is fused with obstacle avoidance using the APF method [4]. In most path planning methods, the robot's platform is considered as a point in the configuration space. However, in this work, the entire surface of the platform is considered for obstacle avoidance (see Fig. 1). The proposed algorithm is able to find the optimal and safe path while projection points of the generated path are entirely in the image boundary. Experiment results show the efficiency of the proposed method for the four-wheel steerable, omnidirectional mobile robot called iMoro [8].

In Section II, we define the proposed path planning problem. Next, in Section III, we explain the requirements for path planning such as the camera model, pose estimation method and obstacle recognition method. Then, in Section V, the robot configuration workspace is explained. Finally, in the Section VI, we show the efficacy of the proposed method through experiments done for the iMoro mobile robot.

II. Problem Definition

In this paper, we propose an obstacle-free path planning algorithm for an omnidirectional mobile robot in order to reach the desired goal configuration, starting from a given initial pose via an overhead camera (see Fig. 2). The initial generated path in the image space can be transformed to the inertial center coordinate of the robot workspace to employ a safe and obstacle-free path for the mobile robot. Based on the APF concepts, we assume the projection points of the mobile robot in the image space are under the influence of the APF to move the mobile robot from one state to another without any collision.

In this case, the robot motion can be interpreted as the motion of the recognized points in the gradient vector field, which is projected in the image space. The field is generated by positive and negative electric points. The vertices have the positive charge in the initial pose and negative charge in the goal pose in the image. Moreover, the recognized points of the obstacles in the image space are set with positive charges. The gradient field in this context can be interpreted as a force that attracts the positively charged mobile robot points to the negative points, which are acting as the goal. The obstacle points and the image border act as a set of positive charges that generate repulsive forces in the image space and push the vertices of the platform away. Hence, the combination of attractive force to the goal and repulsive forces away from the obstacles drives the robot in a safe path to the goal.

To solve the problem based on the APF, we fuse the image-based path planning method with obstacle avoidance approach to generate an obstacle-free path with respect to the camera frame. The visual servoing concepts define the relationship between the generated path in the 2D image space and its corresponding path in the real robot workspace. The generated path can be transformed to the inertial coordinate frame, which has already been recognized as the start point, and it serves as the input to the path follower motion controller [8].

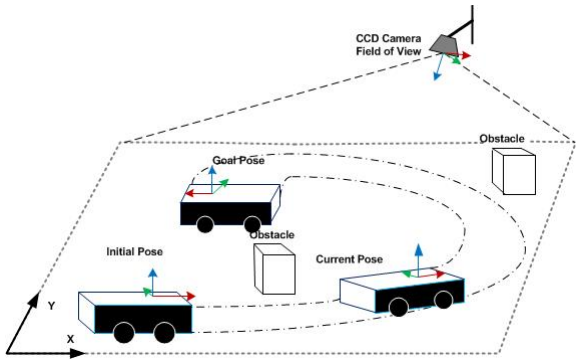

Fig. 2. The problem is finding an obstacle-free-path for the omnidirectional robot when the overhead camera gives the image of its start/stop poses

III. Requirements

A. Distortion-Free Camera Model

Let (x,y,z) represent the coordinate of the mobile robot body center point Q in the world reference W, and let (x_c, y_c, z_c) represent it in the overhead camera workspace W_c (see Fig. 2). The relationship between the world and the camera center coordinate where R is 3×3 rotation matrix, defining the camera rotation, and $T = (t_1, t_2, t_3)$ is a translation vector defining the camera position as

$$\begin{pmatrix} x_c \\ y_c \\ z_c \end{pmatrix} = R \begin{pmatrix} x \\ y \\ z \end{pmatrix} + T. \tag{1}$$

The image plane coordinates of point Q are given by the equations $u = f\frac{x_c}{z_c}$ and $v = f\frac{y_c}{z_c}$, where (u, v) are image plane coordinates, and f is the camera focal length. Geometrical distortion concerns the position of the image point in the image plane. Here, we assume a lens distortion converts the image projection point (u, v) into the $(\widetilde{u}, \widetilde{v})$ via the following relations: $\widetilde{u} = \frac{2u}{1+\sqrt{(1-4K_1(u^2+v^2))}}$, $\widetilde{v} = \frac{2v}{1+\sqrt{(1-4K_1(u^2+v^2))}}$. The transformation points from the image plane coordinates into the image center coordinates system (column, row) in the image space are $c = \frac{\widetilde{u}}{S_x} + C_x, r = \frac{\widetilde{v}}{S_y} + C_y$, where $a^2 = (\widetilde{u}^2 + \widetilde{v}^2)$, and C_x and C_y denote the column and the row of the image center point (center of the radial distortion), respectively. K_1 is the distortion coefficient, and S_x and S_y are the camera scale factors [12].

B. Pose Estimation

Various methods exist for pose estimation from a single image [9], [13]. Here, the 3D position and orientation of the mobile robot are estimated directly from the image using the

available 3D CAD model of the object via the CAD-based recognition approach [9], [14].

First, in the off-line step, a model of our desired object is trained by estimating the range of the poses for every hypothesized pose that may appear in the front of the camera in the 2D model. Moreover, for each 2D model, the corresponding pose is stored. The 2D model created using the similarity measure is robust against occlusion, clutter, and lightening. Next, in the on-line recognition step, the hierarchical view-based approach can be used to recognize the object in an image. Then, for each image found in 2D view, the corresponding object pose is computed by minimizing a geometric distance measure in the image [14]. In this pose-estimation method, the measurement accuracy depends on the distance between the camera and the object. The mean absolute error is the (0.12 - 0.34) percent in position and about (0.3 - 0.5) degree in rotation with respect to the object distance [9].

C. Static Obstacle Recognition with Monocular Vision

The static obstacles in indoor environments have different shapes and colors and may present themselves in many different forms and situations. In many applications, pre calculated data structures can be constructed based on existing information about the environment in order to generate a path around a variety of different static obstacles.

Different monocular vision-based obstacle recognition methods were proposed [15], [16]. However, most monocular vision-based methods detect specific obstacles according to the physical characteristics of the obstacles, such as shape, color, intensity and type of the ground. Collision avoidance requires an accurate separation of obstacles from the background. Image segmentation refers to the process of segmenting the pixels from an image into a region. Here, to specify the obstacle in the image according its color, we employ the Hue-Saturation-Value (HSV) color filter [17]. Its main steps are shown in Fig. 3.

D. Known Target

The omnidirectional mobile robot iMoro has independently steerable wheels that consist of a rigid base and four legs. Each of which has two degrees of freedom (DOF) [18]. The mobile robot is modeled by 2D rigid rectangle translating and rotating in the plane R^2. As illustrated in Fig. 4, $u = \{\hat{X}, \hat{Y}\}$ shows the coordinate frame of the inertial center frame O embedded in the plane. A configuration of the robot body center denoted by Q is defined by the tuple $(\hat{x}, \hat{y}, \theta)$, where x and y are the coordinates of Q. The orientation of the robot denoted by θ is the angle between the $\hat{X}$ of the Cartesian inertial frame embedded in the plane. The $\hat{x}$ axes of the robot body frame follows the generated path denoted by $P(s)$.

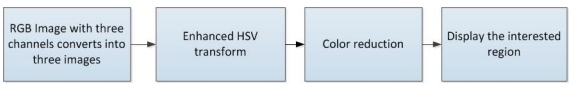

Fig. 3. Image segmentation steps using the HSV filter

In the most often proposed path planning approach, the mobile robot is considered as a point. However, in this research, to reach the planning path from one initial state to another goal state, not only the robot center point Q but also the mobile robot vertices should avoid obstacles. To specify the entire volume of the mobile robot using the CAD model, we employ the CAD-based recognition method, which is explained in SectionIII-B. Q and its projection point Q_{cp} has the similar coordinate frame. The camera model defines the transformation matrix from Q in the real world W to Q_{cp} in the camera workspace W_c. In our presented obstacle-free process, the robot corner points map in the ground to be avoided.

The vertices point of the robot body and also its mapped points in the ground plane with zero height in the real world can be obtained using the following relation: ${}^{Q_i}\mathbf{T}_{Q_{cp}} = [{}^{Q_i}\mathbf{R}_{Q_{cp}}, {}^{Q_i}\mathbf{t}_{Q_{cp}}]$, where $\mathbf{t} \in \Re(3)$ and $\mathbf{R} \in SO(3)$ and $i = 0, 1, \ldots, k-1$. It transforms Q_{cp} to the desired k points belong to the robot wire-frame and its ground corner points in the image space. As illustrated in Fig. 5, the desired points in the ground plane have the similar rotation and different position. The desired vector of image points $\mathbf{s} = \{Q_0, Q_1, ..., Q_4\}$ shows these robot vertices points mapped in the ground.

IV. Mathematical Solution

The influence of the artificial potential field V in the image space is the sum of the two following terms: 1) the attractive potential field V_{at} whose role is to pull the robot toward the goal workspace, and 2) the repulsive potential field V_{rp} whose role is to push the robot away from constraints such as obstacles.

The artificial force $\mathbf{F}(\boldsymbol{\Upsilon}) = -\overrightarrow{\nabla} V$ is the gradient vector of V at direction $\boldsymbol{\Upsilon}$. Therefore, $\mathbf{F}(\boldsymbol{\Upsilon}) = \alpha \mathbf{F}_{at}(\boldsymbol{\Upsilon}) + \beta \mathbf{F}_{rp}(\boldsymbol{\Upsilon})$, where the attractive force is denoted by $\mathbf{F}_{at}(\Upsilon)$, the repulsive force is denoted by $\mathbf{F}_{rp}(\boldsymbol{\Upsilon})$, and $\boldsymbol{\Upsilon}$ is a 6×1 vector representing the parameterization of the robot workspace that is induced by potential fields. Scale factors α and β are used to adjust the influence of repulsive and attractive forces. The

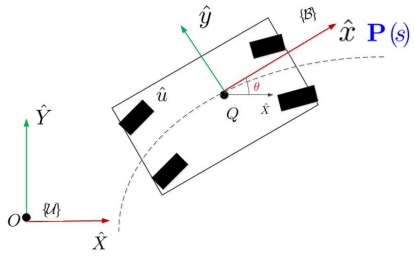

Fig. 4. A view of the mobile robot body frame and its inertial coordinate frame

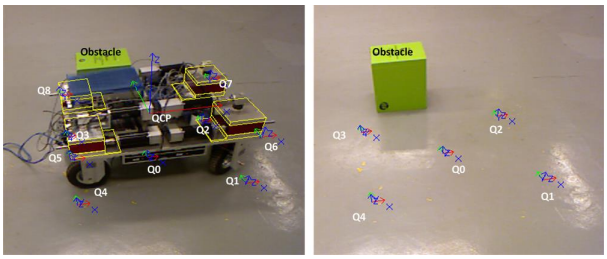

Fig. 5. Image projection points of the robot base frame and its corners, mapped in the ground plane

desired path along the direction of $(\boldsymbol{\Upsilon})$ is obtained as [3]

$$\boldsymbol{\Upsilon}_{k+1} = \boldsymbol{\Upsilon}_k + \epsilon_k \frac{\mathbf{F}(\boldsymbol{\Upsilon}_k)}{\parallel \mathbf{F}(\boldsymbol{\Upsilon}_k) \parallel}, \tag{2}$$

where ϵ_k is a positive scaling factor, and k is an index that increases during the generation of a path. To this end, the homogeneous transformation matrices ${}^{c}\mathbf{T}_{in} = [{}^{c}\mathbf{R}_{in}, {}^{c}\mathbf{t}_{in}]$ and ${}^{c}\mathbf{T}_{de} = [{}^{c}\mathbf{R}_{de}, {}^{c}\mathbf{t}_{de}]$ where $\mathbf{t} \in \Re(3)$ and $\mathbf{R} \in SO(3)$, provide the rotation and translations of the moving object in the initial and the desired poses, respectively.

Our desired parameterization workspace is denoted by $\boldsymbol{\Upsilon}^T = [\mathbf{t}^T, (\mathbf{u}\theta)^T]$, when the initial configuration workspace is denoted by $\boldsymbol{\Upsilon}_{in}^T = [{}^{de}\mathbf{t}_{in}^T, (\mathbf{u}\theta)_{in}^T]$, and the final configuration workspace is denoted by $\boldsymbol{\Upsilon}_{de}^T = 0_{6\times 1}$. Therefore, the vector of our desired workspace $\boldsymbol{\Upsilon}$ can be obtained using the relation

$$\begin{cases} {}^{de}\mathbf{R}_{in} = {}^{de}\mathbf{R}_{c}.{}^{in}\mathbf{R}_{c}^{T} \\ {}^{de}\mathbf{t}_{in} = -{}^{de}\mathbf{R}_{in}.{}^{in}\mathbf{t}_{c} + {}^{de}\mathbf{t}_{c}. \end{cases} \tag{3}$$

A. Attractive Potential Field and Force

The attractive potential field V_a is a parabolic function pulling the robot to the goal configuration to minimize the distance between the current pose and the desired pose in 3D Cartesian workspace [3]. Because we set $\boldsymbol{\Upsilon}_d = \mathbf{0}_{6\times 1}$ as the desired destination of the robot workspace, $V_{at} = \frac{1}{2}\alpha \parallel \boldsymbol{\Upsilon} - \boldsymbol{\Upsilon}_d \parallel^2$ or $V_{at} = \frac{1}{2}\alpha \parallel \boldsymbol{\Upsilon} \parallel^2$ where α is a positive scaling factor. Therefore, the attractive potential force is

$$\mathbf{F}_{at}(\boldsymbol{\Upsilon}) = -\overrightarrow{\nabla} V_{at} = -\alpha \boldsymbol{\Upsilon}. \tag{4}$$

B. Repulsive Potential Field and Force

The goal of the repulsive potential force $\mathbf{F}_{rp}(\boldsymbol{\Upsilon})$ is to push the robot away from the obstacles and visual constraints. Our desired repulsive potential force is the sum of the following two terms : 1) obstacle avoidance potential field and force in the image space,and 2) visibility constraint potential field and force.

1) Obstacle Avoidance Potential Field and Force in the Image Space: To fuse the obstacle avoidance and path planning in the image space, we define an new artificial potential force to push the robot away from the segmented obstacles with an arbitrary shape in the image space. In the mobile robot workspace, there are a number of obstacles. All specified projection points belong to the segmented obstacles in W_c denoted by $\mathcal{O}_i^j = (\widetilde{u}_i, \widetilde{v}_i)^j$, $j = 1, \ldots, n.$ $i = 1, \ldots, m.$, where n is the number of specified obstacles, and m is the number of segmented points belonging to each specified obstacle in W_c. To create the suitable artificial potential force that moves the robot smoothly away from the obstacles in W_c, we use the FIARS repulsive potential function [3]. The desired potential field is defined as

$$V_{rp}^{i}(\mathbf{s}) = \begin{cases} 1/2\eta(1/d_i(p_{min}) - 1/Q_i)^2 & ,if\ d_i(p_{min}) \le Q_i \\ 0 & ,if\ d_i(p_{min}) \ge Q_i, \end{cases} \tag{5}$$

where

$$p_{min} = \arg\min_{p \in \mathbf{s}} d_i(p),$$

and

$$d_i(p) = \left\| \mathcal{O}_i - p \right\|, \ i = 1, \ldots, m.$$

Note that $d_i(p)$ is the influence distance from the i-th point of the obstacle projection points in the image space. Also, η is a positive scaling factor, and Q_i is the range of influence of the function that allows the robot to go sufficiently far away from the obstacle region that belongs to the obstacle segmented points. The final repulsive potential function is the summation of all repulsive potential functions created by all pieces of the obstacle region:

$$V_{rp_{\mathcal{O}}}(\mathbf{s}) = \sum_{i=1}^{m} V_{rp}^{i}(\mathbf{s}) \tag{6}$$

Therefore, the artificial repulsive force or the gradient vector of $V_{rp_{\mathcal{O}}}(\mathbf{s})$ at $\boldsymbol{\Upsilon}$ is

$$\mathbf{F}_{rp_{\mathcal{O}}}(\boldsymbol{\Upsilon}) = -(\frac{\partial V_{rp_{\mathcal{O}}}(\mathbf{s})}{\partial \boldsymbol{\Upsilon}})^T = -(\frac{\partial V_{rp_{\mathcal{O}}}(\mathbf{s})}{\partial \mathbf{s}} \frac{\partial \mathbf{s}}{\partial \mathbf{r}} \frac{\partial \mathbf{r}}{\partial \boldsymbol{\Upsilon}})^T, \tag{7}$$

where:

- $\mathbf{r}$ represents the coordinates of the robot or target point that is moving with respect to the camera frame, and $\dot{\mathbf{r}}$ represents the corresponding mobile robot point velocity in the image space.
- $\dot{\mathbf{s}} = \frac{\partial \mathbf{s}}{\partial \mathbf{r}}$ denoted by $\mathbf{L} = \frac{\partial \mathbf{s}}{\partial \mathbf{r}}$ is the Jacobian matrix and defines how image points $\mathbf{s}$ change with respect to the camera frame. Here, we have the lens distortion that is described in Section III-A. Therefore, rewrite the linearized Jacobian matrix as

$$\mathbf{L}(\mathbf{p}_i, \mathbf{z}) = \begin{bmatrix} \frac{f}{z} & 0 & -\frac{\widetilde{u}_i}{z} & -\frac{\widetilde{u}_i\widetilde{v}_i}{f} & -\frac{f^2+\widetilde{u}_i^2}{f} & -\widetilde{v}_i \\ 0 & \frac{f}{z} & -\frac{\widetilde{v}_i}{z} & -\frac{f^2+\widetilde{v}_i^2}{f} & -\frac{\widetilde{u}_i\widetilde{v}_i}{f} & \widetilde{u}_i \end{bmatrix}, \tag{8}$$

where the robot points in the world coordinates are moving in front of the camera. The Jacobian matrix for image vector $\mathbf{s}$ composed of the mapped center point Q_0 and k projection points $Q_i = (\widetilde{u}, \widetilde{v})$ is calculated as follows:

$$\mathbf{L}(\mathbf{s}, \mathbf{z}) = [\mathbf{L}^T(Q_0, z_0) ... \mathbf{L}^T(Q_k, z_k)]^T \tag{9}$$

• $\mathbf{M}_{\boldsymbol{\Upsilon}} = \frac{\partial \mathbf{r}}{\partial \boldsymbol{\Upsilon}}$ is the variation of $\mathbf{r}$ to the variation of trajectory workspace with respect to camera frame $\boldsymbol{\Upsilon}$ as

$$\mathbf{M}_{\boldsymbol{\Upsilon}} = \begin{bmatrix} {}^{de}\mathbf{R}_{in}^{T} & \mathbf{0}_{3\times 3} \\ \mathbf{0}_{3\times 3} & \mathbf{L}_{w}^{-1} \end{bmatrix}, \tag{10}$$

where, $\mathbf{L}_{w}^{-1} = I_{3\times 3} + \frac{\theta}{2} sinc^2(\frac{\theta}{2})[u]_{\wedge} + (1 - sin(\theta))[u]_{\wedge}^2$ was defined using visual servoing concepts [10]. Also, u is the rotation axis, and θ the rotation angle obtained from rotation $\mathbf{R}$ between the initial pose and the desired pose with respect to the camera frame. The $u\theta$ can be expressed as a function of the robot velocity with respect to the camera frame.

• $\mathbf{O}_{\mathcal{O}}(\mathbf{s}) = (\frac{\partial V_{rp_{\mathcal{O}}}(\mathbf{s})}{\partial \mathbf{s}})$ is a variation of the repulsive potential function obtained from Equations (5) and (6) to the variation of the vector $\mathbf{s}$, composed of k projection points of the moving object. It defines how the repulsive potential function changes near the robot projection points in W_c. In other words repulsive force $\mathbf{O}_{\mathcal{O}}(s)$ pushes the vector $\mathbf{s}$ away from all points of the obstacles already segmented in W_c. Therefore, the desired obstacle avoidance potential force is

$$\mathbf{F}_{rp_{\mathcal{O}}}(\Upsilon) = -\mathbf{M}_{\boldsymbol{\Upsilon}}^{T}\mathbf{L}^{T}\mathbf{O}_{\mathcal{O}}^{T}. \tag{11}$$

2) Visibility Constraints Repulsive Potential Field and Force: A visibility constraint implies a potential barrier function to push the mobile robot to reach the goal state while remaining in the camera's field of view. The limits of 2D image space are defined by $[u_m, u_M]$ and $[v_m, v_M]$. When the extracted wire-frame points $\mathbf{s}$ reach near the limits, a repulsive force will be generated to push them away from the image limits. The repulsive potential function $V_{rp\mathcal{V}}(\mathbf{s})$ for $\mathbf{s}$ is introduced in [10] as

$$V_{rp\mathcal{V}}(s) = -\ln(\prod(1 - \frac{\widetilde{u_i}}{u_m})(1 - \frac{\widetilde{u_i}}{u_M})(1 - \frac{\widetilde{v_i}}{v_m})(1 - \frac{\widetilde{v_i}}{v_M})).$$

$$\begin{cases} V_{rp\mathcal{V}}(\mathbf{s}) & \text{if } \mathbf{s} \in \mathcal{C} \\ 0 & \text{Otherwise,} \end{cases} \tag{12}$$

where $\mathcal{C}$ is the set of acceptable image projected points, considering the lens distortion, $\mathcal{C} = \{s/\exists_j(\widetilde{u_i}, \widetilde{v_i})|\widetilde{u_i} \in (u_m - \alpha_d, u_M - \alpha_d), \widetilde{v_i} \in (v_m - \alpha_d, v_M - \alpha_d)\}$, α_d is a positive constant represent the influence of distance for the image edges in pixels. The function $V_{rp\mathcal{V}}(\mathbf{s})$ tends to infinity when at least one extracted image point of the wire-frame gets closer to the image limits. Furthermore, it is null if all extracted wire-frame points are sufficiently far away from the image limits. The artificial repulsive force is the gradient vector of $V_{rp\mathcal{V}}(\mathbf{s})$ at the current workspace $\boldsymbol{\Upsilon}$ as

$$\mathbf{F}_{rp\mathcal{V}}(\boldsymbol{\Upsilon}) = -(\frac{\partial V_{rp\mathcal{V}}(\mathbf{s})}{\partial \boldsymbol{\Upsilon}})^T = -(\frac{\partial V^{Vis}(\mathbf{s})}{\partial \mathbf{s}} \frac{\partial \mathbf{s}}{\partial \mathbf{r}} \frac{\partial \mathbf{r}}{\partial \boldsymbol{\Upsilon}})^T,$$

where, $\mathbf{L}_s = \frac{\partial \mathbf{s}}{\partial \mathbf{r}}$, and $\mathbf{M}_{\boldsymbol{\Upsilon}} = \frac{\partial \mathbf{r}}{\partial \boldsymbol{\Upsilon}}$ already were defined in Equation (10). The function $V_{rp\mathcal{V}}$ is positive or null tending to infinity when at least one selected image point gets closer to the image limits, and it is null when all image points are far away from the image limits, sufficiently. $\mathcal{V}_{\mathbf{s}} = \frac{\partial V_{rp\mathcal{V}}(\mathbf{s})}{\partial \mathbf{s}}$ can be calculated simply. Therefore, $F_{rp\mathcal{V}}(\boldsymbol{\Upsilon})$ is

$$\mathbf{F}_{rp\mathcal{V}}(\boldsymbol{\Upsilon}) = -(\mathcal{V}_{\mathbf{s}}\mathbf{L}_s\mathbf{M}_{\boldsymbol{\Upsilon}})^T. \tag{13}$$

3) Total Repulsive Potential Fields and Forces: The final repulsive potential field is composed of the obstacle avoidance repulsive potential field and visibility constraints repulsive potential field, via Equations (6) and (12). The total repulsive force is given by

$$\mathbf{F}_{rp}(\boldsymbol{\Upsilon}) = \mathbf{F}_{rp\mathcal{V}}(\boldsymbol{\Upsilon}) + \mathbf{F}_{rp\mathcal{O}}(\boldsymbol{\Upsilon}). \tag{14}$$

V. CONFIGURATION WORKSPACE

A desired path along the direction of the artificial potential force is calculated via Equation (2). The generated vector induced by potential function $\boldsymbol{\Upsilon}_i = [\mathbf{t}_i, (\mathbf{u}\theta)_i]_{i=0}^{k}$ represents the mobile robot parameterization workspace. Transformation of the k-th generated 3D path to the camera workspace can be obtained via the following equations:

$$\begin{cases} {}^{c}\mathbf{R}_k = {}^{k}\mathbf{R}_{de}^{T}.{}^{c}\mathbf{R}_{de} \\ {}^{c}\mathbf{t}_k = {}^{k}\mathbf{R}_{de}^{T}({}^{c}\mathbf{t}_{de} - {}^{de}\mathbf{t}_k). \end{cases} \tag{15}$$

We assume this projected point Q_0 is the inertial coordinates center of the mobile robot denoted O. The k-th generated path can be transformed to O, via the following relation:

$$\begin{cases} {}^{O}\mathbf{R}_k = {}^{c}\mathbf{R}_{O}^{T}.{}^{c}\mathbf{R}_k \\ {}^{O}\mathbf{t}_k = {}^{c}\mathbf{R}_{O}^{T}.({}^{c}\mathbf{t}_k - {}^{c}\mathbf{t}_O). \end{cases} \tag{16}$$

The generated path shows the 3D position and 3D orientation of the mobile robot with respect to its initial frame O. The mobile robot moves in the flat surface; therefore, the desired mobile robot 2D path $P(\mathbf{s})$, where $\mathbf{s} = [Q_0, ..., Q_{k-1}]^T$, can simply be obtained from the generated 3D path. The Cubic B-spline interpolation method can be employed to interpolate the generated path to the form of the curve and adjust it to ensure the motion constraint will be satisfied throughout the robot motion.

VI. EXPERIMENT RESULTS

To test our proposed obstacle-free path planning method, several experiments were performed. The results of two setups A, B with omnidirectional robot iMoro are presented. The dimensions of the robot are known, and its CAD model is available. The CAD center coordinates coincide in the robot body center point. Two grabbed images by the calibrated overhead camera give the global position of the robot in the initial and the desired configuration workspace (see Fig. 6 for setup A and Fig. 7 for setup B). The 3D position and orientation of the robot are estimated using the CAD-based recognition method. Here, the projection of the robot-body frame and its vertices points mapped in the ground give the image vector $\mathbf{s} = [Q_0, ..., Q_4]^T$. The existing

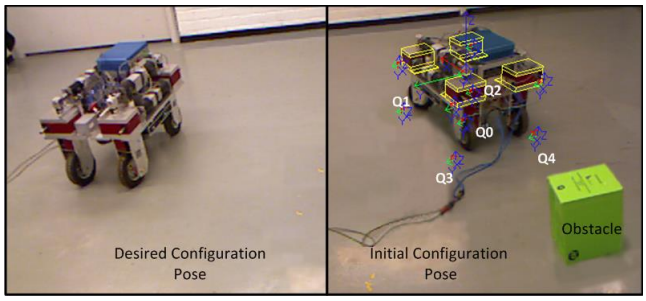

Fig. 6. Setup A, start point (right) and stop point (left)

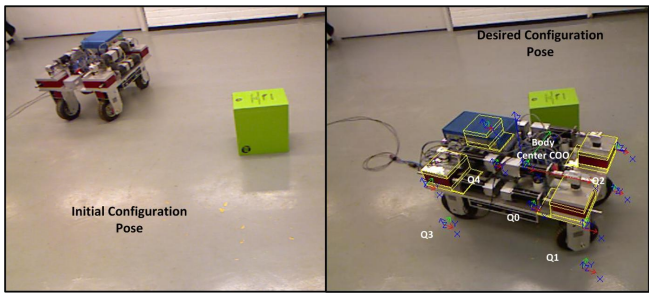

Fig. 7. Setup B, start point (left) and stop point (right)

obstacle projection point $\mathcal{O}_i^j,\ j = 1,\ldots,n.\ i = 1,\ldots,m$, is segmented using the HSV filter.

The goal is planning an obstacle-free path $P(\mathbf{s})$ in the horizontal plane for iMoro. Setup A is tested to generate the desired path to avoid the segmented obstacle in the image space and the image boundary. Setup B shows the effect of the field of view or image boundary constraint to push the robot away from the camera field of view during the planning of a path. The vector $\boldsymbol{\Upsilon}_{i=0}^{k}$ generates and its position and orientation in the Cartesian workspace are illustrated in Fig. 8 and Fig. 9. The generated obstacle-free path with respect to the camera frame for setup A and setup B are shown in Fig. 10. We transform it to the inertial frame of the robot which has already estimated, for both setups (see Fig. 11). These generated paths give direction (x, y) of the robot body frame Q_0 and its angle θ from the start point to the goal (see Fig. 12).

VII. Conclusion

This paper proposes global path planning for mobile robots using a single overhead camera. Two types of obstacles are avoided. The first type is the static objects, which are recognized in the image space. The second type is the image boundary that acts as an obstacle. The latter keeps the generated path always in the camera field of view and hence guarantees that robot stays in the visibility range of the overhead camera. This has been done by fusing the obstacle-avoidance method extended in the image space and an extension of the image-based path planning integrated by the CAD-based recognition method. In our future work, we hybrid the current work with the local path planning based on the APF for an omnidirectional mobile robot.

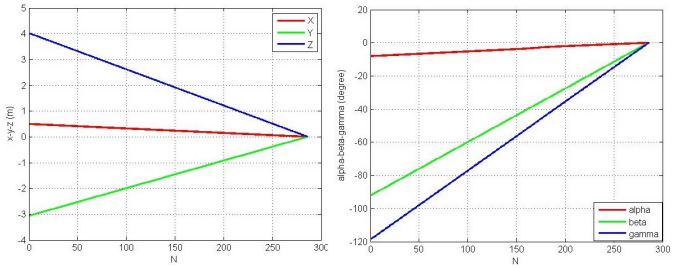

Fig. 8. Setup A, the vector $\boldsymbol{\Upsilon}_{i=0}^{280}$ position (left) and orientation (right)

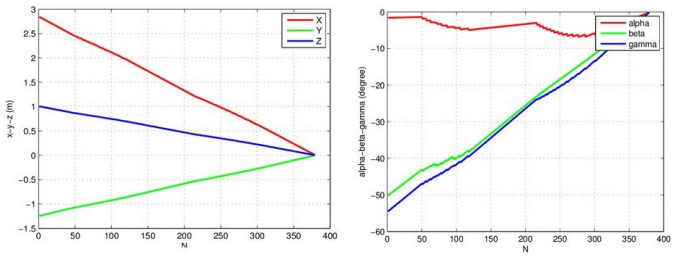

Fig. 9. Setup B, the vector $\boldsymbol{\Upsilon}_{i=0}^{380}$ position (left) and orientation (right)

References

[1] V. Kunchev, L. Jain, V. Ivancevic, and A. Finn, "Path planning and obstacle avoidance for autonomous mobile robots: A review," in *Knowledge-Based Intelligent Information and Engineering Systems*. Springer, 2006, pp. 537–544.

[2] N. Buniyamin, N. Sariff, W. Wan Ngah, and Z. Mohamad, "Robot global path planning overview and a variation of ant colony system algorithm," *International journal of mathematics and computers in simulation*, vol. 5, no. 1, pp. 9–16, 2011.

[3] O. Khatib, "Real-time obstacle avoidance for manipulators and mobile robots," *The international journal of robotics research*, vol. 5, no. 1, pp. 90–98, 1986.

[4] C. W. Warren, "Global path planning using artificial potential fields," in *Robotics and Automation, 1989. Proceedings., 1989 IEEE International Conference on*. IEEE, 1989, pp. 316–321.

[5] J. Carsten, A. Rankin, D. Ferguson, and A. Stentz, "Global path planning on board the mars exploration rovers," in *Aerospace Conference, 2007 IEEE*. IEEE, 2007, pp. 1–11.

[6] R. S. Rao, V. Kumar, and C. J. Taylor, "Planning and control of mobile robots in image space from overhead cameras," in *Robotics and Automation, 2005. ICRA 2005. Proceedings of the 2005 IEEE International Conference on*. IEEE, 2005, pp. 2185–2190.

[7] W. Huang, A. Osothsilp, and F. Pourboghrat, "Vision-based path planning with obstacle avoidance for mobile robots using linear matrix inequalities," in *Control Automation Robotics & Vision (ICARCV), 2010 11th International Conference on*. IEEE, 2010, pp. 1446–1451.

[8] R. Oftadeh, M. M. Aref, R. Ghabcheloo, and J. Mattila, "Bounded-velocity motion control of four wheel steered mobile robots," in *Advanced Intelligent Mechatronics (AIM), 2013 IEEE/ASME International Conference on*. IEEE, 2013, pp. 255–260.

[9] M. Ulrich, C. Wiedemann, and C. Steger, "Combining scale-space and similarity-based aspect graphs for fast 3d object recognition," *Pattern Analysis and Machine Intelligence, IEEE Transactions on*, vol. 34, no. 10, pp. 1902–1914, 2012.

[10] Y. Mezouar and F. Chaumette, "Path planning in image space for robust visual servoing," in *Robotics and Automation, 2000. Proceedings. ICRA'00. IEEE International Conference on*, vol. 3. IEEE, 2000, pp. 2759–2764.

[11] Z. Ziaei, R. Oftadeh, and J. Mattila, "New scheme for image space path planning incorporating cad-based recognition methods for visual servoing," in *Robotics, Automation and Mechatronics (RAM), 2013 6th IEEE Conference on*. IEEE, 2013, pp. 212–217.
[12] Z. Ziaei, A. Hahto, J. Mattila, M. Siuko, and L. Semeraro, "Real-time markerless augmented reality for remote handling system in bad viewing conditions," *Fusion Engineering and Design*, vol. 86, no. 9, pp. 2033–2038, 2011.
[13] D. F. DeMenthon and L. S. Davis, "Model-based object pose in 25 lines of code," in *Computer VisionECCV'92*. Springer, 1992, pp. 335–343.
[14] http://www.mvtec.com/halcon/.
[15] S. Lenser and M. Veloso, "Visual sonar: Fast obstacle avoidance using monocular vision," in *Intelligent Robots and Systems, 2003.(IROS 2003). Proceedings. 2003 IEEE/RSJ International Conference on*, vol. 1. IEEE, 2003, pp. 886–891.
[16] I. Ulrich and I. Nourbakhsh, "Appearance-based obstacle detection with monocular color vision," 2000.
[17] S. Sural, G. Qian, and S. Pramanik, "Segmentation and histogram generation using the hsv color space for image retrieval," in *Image Processing. 2002. Proceedings. 2002 International Conference on*, vol. 2. IEEE, 2002, pp. II–589.
[18] R. Oftadeh, R. Ghabcheloo, and J. Mattila, "A novel time optimal path following controller with bounded velocities for mobile robots with independently steerable wheels," in *Intelligent Robots and Systems (IROS), 2013 IEEE/RSJ International Conference on*. IEEE, 2013, pp. 4845–4851.

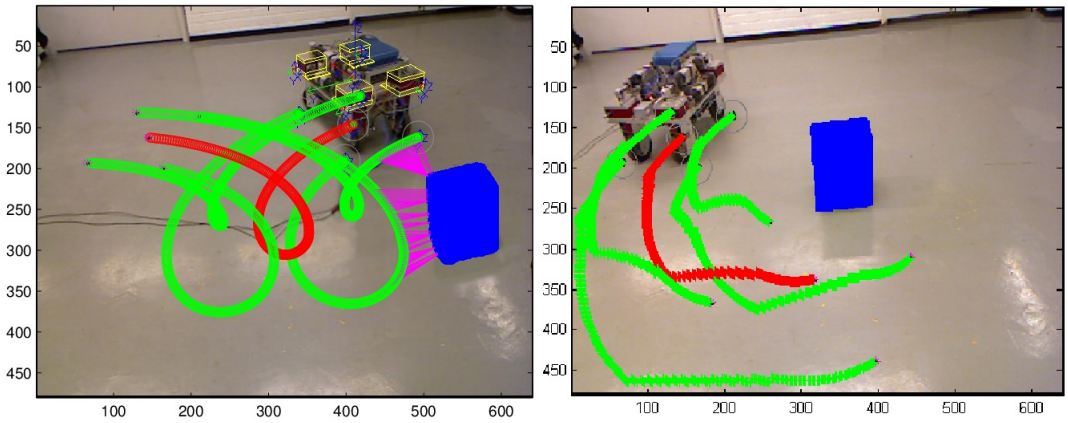

Fig. 10. 2D obstacle-free path in the image space for setup A (left) and setup B (right)

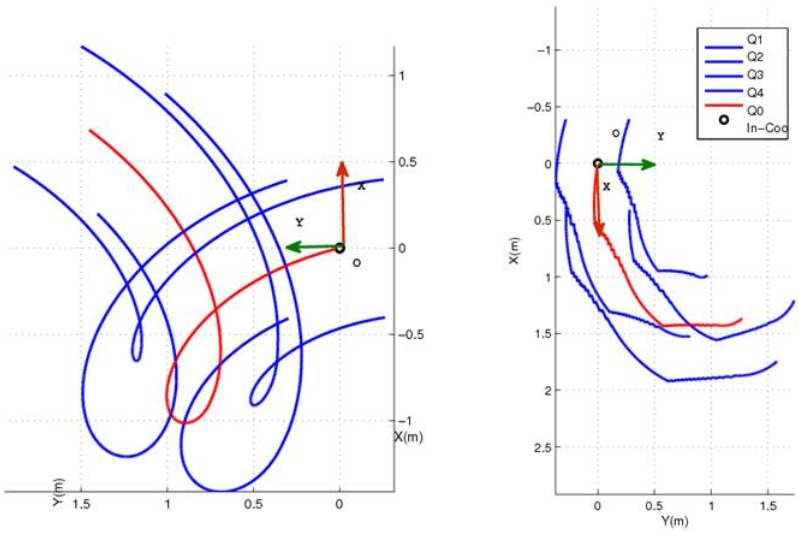

Fig. 11. The generated path transformed to the inertial frame for setup A (left) and setup B (right).

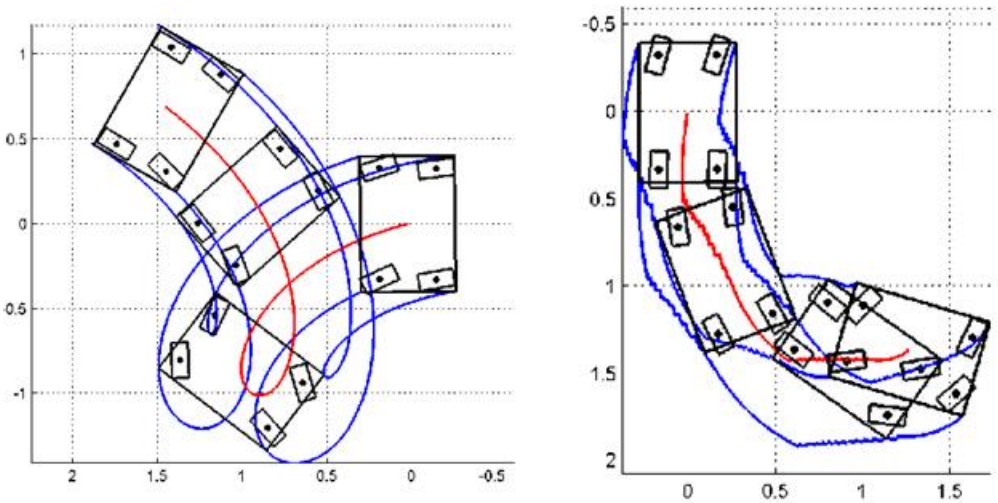

Fig. 12. The Generated paths that results in the robot base position (x, y) and its angle θ in the robot workspace. Setup A (left) and setup B (right)